

Impact of fuel diversification on humidified micro gas turbine potential: A thermodynamic performance assessment

Ward De Paepe^{1*}

1 University of Mons (UMONS), Thermal Engineering and Combustion Research Unit, Mons, Belgium (*Corresponding Author)

ABSTRACT

Cycle humidification is an interesting and effective tool to increase the operational flexibility of micro Gas Turbines (mGTs). However, considering the future fuel diversification towards emission reduction and security of supply, it is essential to identify what the impact of the fuel is on the potential for cycle humidification. To determine this impact, in this paper, we present the results of a black box analysis towards this identification, using 2nd law analysis. Additionally, several advanced humidified cycles concepts have been simulated to assess their sensitivity towards fuel alteration. Black box results indicated that going towards hydrogen has no major impact on the cycle performance, while syngas clearly limits the potential: only injection up to 106 g/s is possible compared to the 123 g/s in the hydrogen case, leading to reduced electric efficiency of 38% compared to the 41% in the latter case. A similar observation was made when considering the specific humidified cycles, where the preheated water injection option showed to be the best performing cycle. For all cases, however, using syngas led to a reduced cycle performance. Finally, none of the cycles could exploit the full black box potential and hence future work consists in the identification of the impact of fuel alteration on the more advanced humidified cycles, in an attempt to reach the full potential.

Keywords: fuel diversification, micro gas turbine, humidification, exergy analysis, black box analysis, 2nd law analysis

NOMENCLATURE

Abbreviations

GT	Gas Turbine
HRSG	Heat Recovery Steam Generator
LHV	Lower Heating Value
mGT	Micro Gas Turbine
mHAT	Micro Humid Air Turbine
STIG	STeam Injected Gas turbine

TIT	Turbine Inlet Temperature
TOT	Turbine Outlet Temperature
<i>Symbols</i>	
<i>Ex</i>	Exergy content (kW)
<i>Subscripts</i>	
dest	Destruction
eff	Efficiency
fuel	Of the fuel
in	Of the ingoing streams
out	Of the outgoing streams
gain	Streams that gain exergy
loss	Streams that lose exergy

1. INTRODUCTION

In the quest towards net zero-carbon emissions in combination with current geopolitical tensions, fuel diversification is essential for our security of supply. Different pathways, including power-to-fuel, where excess renewable energy is stored under the form of hydrogen, or the use of bio-fuels, e.g., syngas, are currently studied. Within this framework, micro Gas Turbines (mGTs) present large potential for the (re)conversion of these fuels in electricity in a decentralized, small-scale cogeneration context, considering their high combined heat and power efficiency, their low emissions, low vibrations and low maintenance cost and mostly their fuel flexibility [1]. However, despite their potential, the limited operational flexibility of mGTs (mainly fixed heat-to-power ratio), remains a major disadvantage.

Cycle humidification is an effective measure to allow for more operational flexibility. By introducing heated water/steam (autoraised using the heat available in the flue gases), part of the waste heat can be recovered in the cycle, leading to higher electric performance, and thus enhanced operational flexibility. This option, first proposed on large scale Gas Turbines (GTs) [2] has already been studied largely on different mGTs, clearly showing its potential [3]. Despite the proven potential, both experimentally [4, 5] and economically [6, 7], so far,

all studies were limited to the use of natural gas. The impact of the use of hydrogen (or hydrogen blends) as well as low calorific fuels (i.e., syngas) on the potential and performance of humidified mGTs is still unknown.

To address this need, in this paper, the results of an in-depth thermodynamic performance analysis of humidified mGTs operating using different fuels is presented. First, the potential for maximized waste heat recovery and thus maximized electric efficiency increase through humidification is found using a black box approach and application of first and second law of thermodynamics. Second, the specific performance of several well-known humidified mGT cycles, including direct preheated water injection, steam injection (STIG) and the micro Humid Air Turbine (mHAT) were identified to assess the impact of the fuel alteration on the cycle performance. Hence, the main novelty of this paper is the assessment of the potential of humidification towards waste heat recovery in mGTs cycles, operating on alternative fuels.

The paper is structured as follows: first the used modelling approach in Aspen Plus is presented, including mGT modelling, black box analysis and humidified cycle concepts presentation and modelling. Second, the results are presented, including first the maximal potential followed by the specific humidified cycles performances. Finally, a conclusion with future perspective is presented.

2. METHODOLOGY

The methodology used for the determination of the potential of humidified mGTs operating on different fuels is based on previous work of the author and consists in 2 steps: first the potential of the humidification is determined using a black box approach [8, 9]. Second, the black box is replaced with an actual heat exchanger network and water introduction method [10]. Both parts are explained in more detail in the next sections, including also a brief description of the considered mGT. Finally, it is important to note that all simulations have been conducted in Aspen Plus v12.

2.1 Turbec T100 mGT

The mGT system considered for the assessment of the potential of humidification in mGTs with different fuels in this paper, is the Turbec T100 mGT (currently commercially available as the AE-T100). This Turbec T100 is a typical mGT, operating according to the recuperated Brayton Cycle (*Figure 1*): Air enters the system via the variable speed centrifugal compressor to increase the pressure up to 4 bars (1). Before entering the combustion chamber, this compressed air is preheated in the recuperator (2) using the heat from the flue gases.

In the combustion chamber (3), fuel is burned until the maximal Turbine Inlet Temperature (TIT) is reached. While expanding over the turbine (4), mechanical power is delivered to drive both the compressor and the high-speed generator (5). Finally, after exiting the recuperator, the remaining heat of the flue gases is converted into thermal power in the economizer (6) under the form of heated water (or steam in some case).

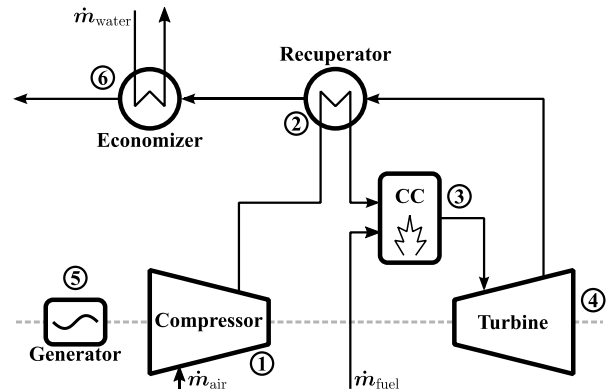


Figure 1: The considered mGT in this paper is the Turbec T100.

The Turbec T100 has a nominal electric power output of 100 kW_e and corresponding 30% electric efficiency, while the thermal power output accounts for 165 kW_{th} and corresponding 50% efficiency (total efficiency of the system accounts for 80%). The unit operates at constant power output, set by the operator, by altering the rotational speed of both compressor and turbine (and thus the mass flow rate entering the system). To ensure maximal electric efficiency, even at part load, a second control action will vary the injected fuel flow rate in the combustion chamber, aiming to keep TIT at its maximal value of 950°C. Considering that it is challenging to measure TIT, the actual control system uses the measurements of the Turbine Outlet Temperature (TOT) and fixed tables to link both TIT and TOT.

The Turbec T100 is simulated in Aspen Plus as follows: for the compressor, it was opted to use the actual map provided by the manufacturer [11], allowing to correctly capture the component off-design behavior. The combustion chamber is modelled using a Gibbs-reactor, ensuring complete combustion. An additional 5% pressure loss and 10 kW_{th} heat loss are included in this component. For the turbine, to ensure fast convergence of the model, rather than using the actual operating map, this component was assumed to be choked (similar assumption was already used successfully by the author of this paper to simulate the impact of steam injection in the mGT [12]), although the choking constant was updated accordingly the altering

inlet conditions when humidification was assumed. The isentropic efficiency was altered based on the composition of the flue gases, using the approach of Parente et al. [13]. For the generator, a 94% efficiency was assumed, while for the turbine and compressor, 99% mechanical efficiency was assumed. For the recuperator, rather than assuming an actual surface and heat exchange coefficient determined based on the NTU method, it was opted to only consider a constant hot pinch of 50°C for a correct comparison of the different cycles.

To study the impact of fuel diversification on the system, 3 types of fuel have been considered in this paper: pure methane (Lower Heating Value – LHV=50 MJ/kg), hydrogen (LHV=120 MJ/kg) and syngas (composition: 55.1% CO, 31.8% CO₂, 7.8% H₂O, 3.8% H₂ and 1.4% CH₄ mass based, LHV = 10.8 MJ/kg). All fuel is injected in the combustion chamber at 30°C and 6 bar. For all simulations, the TIT was considered constant at 950°C, which was achieved by altering the injected mass flow rate using a *Design Spec* in Aspen. Finally, the constant power output control was also activated, assuming 100 kW_e output, using a second *Design Spec* in Aspen, which alters the air entering the cycle.

2.2 Black box approach

To determine the impact of the fuel on the potential of the humidified mGTs, a black box analysis was performed. This black box approach, initially proposed by Bram et al. [8] for large scale GTs and later applied by the author of this paper on mGT scale [9, 14] consists in replacing all heat exchangers from the gas turbine and replacing them with a black box. Over this black box, only first and second law are expressed: first law ensures that no energy is created or destructed in the black box, while the second law ensures that the heat transfer will happen spontaneously and in the correct direction. This is done by imposing a minimal exergy destruction BB_{dest} and maximal exergy efficiency BB_{eff} , which are expressed as:

$$BB_{dest} = \frac{\sum_{in} \dot{E}x - \sum_{out} \dot{E}x}{\dot{E}x_{fuel}} \quad (1)$$

$$BB_{eff} = \frac{\sum_{gain} \Delta \dot{E}x}{\sum_{loss} \Delta \dot{E}x} \quad (2)$$

The black box destruction represents thus the ratio of the difference between in and outgoing exergy flows in the control volume, rated by the introduced chemical exergy of the fuel in the combustion chamber of the mGT. This destruction is set to minimal 5%, to ensure that the obtained performance can be accomplished

with an actual heat exchanger network [9]. The black box efficiency on the other hand, presents the ratio between the exergy of the streams that gain exergy over the streams that lose exergy. Again, to ensure a technical feasible potential, exergy efficiency is limited to 92% [9].

In Aspen Plus, considering that no black box component is available, the black box was simulated using the same approach as presented first in [15]: The heat exchanger network was replaced by a generic HEATER (*Heater* in *Figure 2*) to represent the heating of the cold air coming from the mGT compressor, that is humidified and is going towards the combustion chamber, while a second HEATER (*Cooler* in *Figure 2*), is responsible for the cooling of the hot flue gases, exiting the turbine. To ensure that the first law is respected in the black box, all heat extracted in the cooler, is transferred, and absorbed again in the heater. Finally, the physical exergy content of each stream is determined using the property set *EXGRFL*, while the chemical energy input was determined using the procedure described by Bram et al. [8].

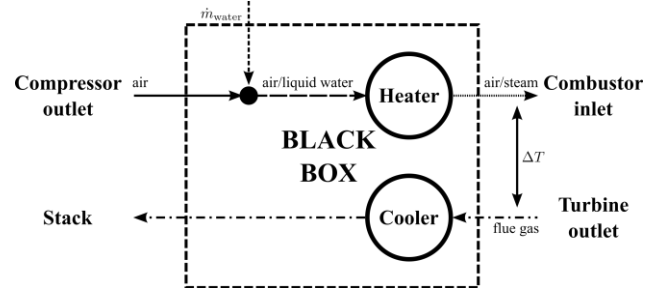


Figure 2: The Black Box as introduced in Aspen Plus, composing of a generic Heater, Cooler and water injection.

To obtain the maximal potential for humidification, the amount of introduced water is gradually increased, while evaluating each time the exergy destruction and efficiency of the black box. Once the limit of one (or both) of them is reached, the maximal potential is found. Given that there is an additional degree of freedom in the system, the hot pinch (temperature difference between the hot flow exiting the turbine and the cold flow going in the combustion chamber) was set to 50°C, a typical value for gas-gas heat exchangers. Furthermore, a 5% and 0.5% pressure loss have been considered for the heater and the water injection respectively, while a 40 mbar pressure loss was assumed for the cooler. Finally, the water is assumed to enter the system at 15°C and 0.5 bar higher pressure than the air.

2.3 Specific humidified mGT cycles

Once the potential for humidified under different fuels is assessed, the performance of different humidified cycles was evaluated and compared to this

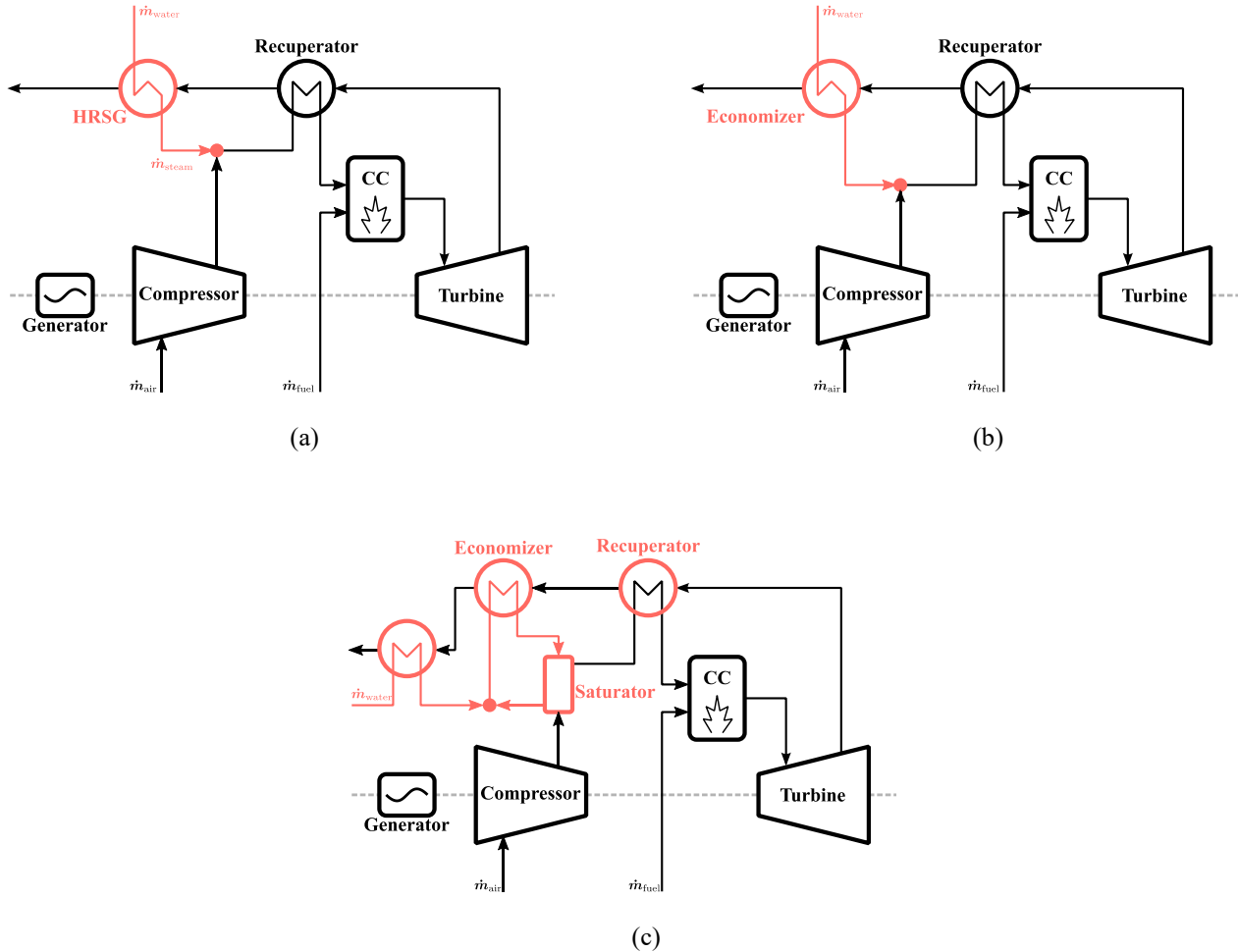


Figure 3: Considered advanced humidified mGT cycles, including STIG (a), preheated water injection (b), and mHAT (c) layout

potential. Considering the large variety of cycles, ranging from simple water injection to the more complex REVAP [16] or M-power [17] cycles, an a priori selection of layouts was performed. At this stage, it was opted to limit the simulated cycles to the simpler cycles, that have already been widely studied numerically and experimentally tested on existing mGTs. Moreover, only cycles having a water introduction between the compressor outlet and a recuperator inlet have been selected, considering their potential for waste heat recovery and performance improvement, while cycles proposing water/steam injection before the compressor in the combustion chamber have been excluded (for a deeper discussion, the author refers to [18]). Finally, the considered cycles include (Figure 3):

- Auto raised steam injection or STIG (a)
- Preheated water injection (b)
- Micro Humid Air Turbine or mHAT [19] (c)

The more advanced cycles will be simulated in a later stage.

In terms of cycle layout, the first two options, including preheated water injection and STIG layout are similar, however, in the preheated water layout, the liquid water is heated till below its saturation point and enters the mGT between the compressor outlet and the recuperator in its liquid state, while in the STIG layout, the economizer is replaced with a Heat Recovery Steam Generator (HRSG), producing saturated steam, and injecting it in the compressor outlet.

For the preheated water injection case, 2-specific cases have been considered: water injection up to full saturation before the recuperator (so 100% relative humidity and no liquid water entering the recuperator) and maximal water injection, leading to fully saturated compressed air, but also liquid water entering the recuperator. This distinction was made, considered that the first case has no specific technological challenges, while the latter case, exploiting 2-phase flow in the cycle,

can be technologically challenging toward design, control, and operation.

The last considered cycle is the mHAT. While the first 2 consists in cycles where all injected water is evaporated and goes through the cycle, in the mHAT cycle (based on the HAT cycle, which was first proposed by Rao et al. [20]), water is introduced in a saturation tower with a large excess. Only part (up to 4%) of this water is evaporated in the compressed air, extracting its heat for evaporation from the remaining water. Finally, the excess water is leaving the tower at a lower temperature than when entering and extracts additional waste heat from the flue gases in the economizer. To ensure for a constant amount of circulating water, feedwater is entering the cycle (first being preheated).

For the determination of the potential of each cycle, similar assumptions as for the black box simulations have been considered: the water introduction part introduces a 0.5% pressure loss, while the recuperator has a 5% pressure loss on the high-pressure side and a 40 mbar pressure loss on the low pressure side. In this recuperator, a 50°C pinch was assumed (typical for gas-gas heat exchangers), while in the economizers, HRSG and preheaters, 10°C pinch was assumed (typical for gas-liquid heat exchangers). Feedwater enters the system at 15°C and 0.5 bar higher pressure compared to the compressed air pressure. Finally, the mGT components and controls (constant power and TIT) were similar as in the dry mGT and the black box simulations.

3. RESULTS

In this section, first the impact of fuel alteration on the dry cycle is presented, followed by the black box results and finally the specific advanced humidified cycle performance.

3.1 Dry mGT results

As presented in *Table 1*, switching from methane to pure hydrogen as fuel has an almost negligible impact on the cycle performance (difference of 0.2%abs on the efficiency), which can be explained by the slightly higher heat capacity of the flue gases because of the increasing water content after the combustion of hydrogen. Considering that the mGT operates rather lean with a large excess of air, this effect is only limited. Due to this higher heat capacity, in combination with the lower fuel mass flow rate, the rotation speed (and thus the air mass flow rate) can be lowered by the control system, while still operating at constant power.

Switching to syngas has a more distinct, negative impact on the cycle performance. Not only does the syngas have a significant larger mass flow rate (explaining the drop in rotational speed and air mass flow

Table 1: Altering between CH₄ and H₂ has only a minor effect on the mGT performance, while syngas leads to a significant performance reduction. Simulations taken at constant power output (100kW_e)

FUEL TYPE	m _{air} (g/s)	m _{fuel} (g/s)	η _{el} (%)	n (Hz)
CH ₄	710	6.09	32.8	1122
H ₂	700	2.52	33.0	1113
SG	675	29.00	31.9	1109

rate at constant power output), but the large dilution also due to the presence of large fraction of CO₂ and to a lesser extend of H₂O has a negative impact on the mGT performance, leading to an electric efficiency reduction of 0.9%abs.

3.2 Black Box analysis

A first parameter to consider when analyzing the black box analysis is the electric efficiency (*Figure 1*), especially given that the final aim of humidification is the recovery of waste heat to increase the cycle electric efficiency. For all different fuels, increasing the water injection flow rate leads to higher waste heat recovery and higher efficiency. Although in absolute values, there is a distinct difference between the use of low calorific fuels, i.e., syngas, compared to higher calorific fuels, like hydrogen and methane, the relative change in efficiency is similar for all fuels. However, for the syngas case, only a reduced amount of water (106 g/s) could be introduced in the cycle, which is remarkable lower compared to the hydrogen case (122 g/s) and the methane case (123 g/s). Comparing these last 2 cases, there is indeed a slightly higher potential in the methane case (1 g/s), but in the opinion of the author, this can be neglected, considering that this is within the accuracy of the solver. Finally, it is important to note that, although under dry conditions, the hydrogen had a slightly higher electric efficiency compared to the methane case, as a result of the higher

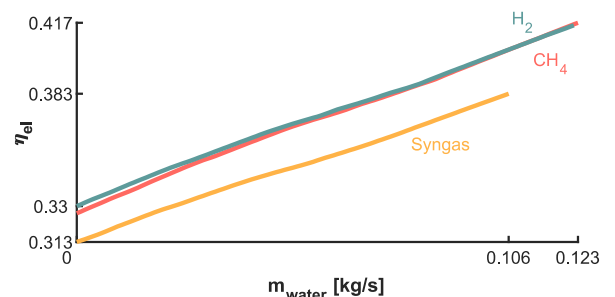


Figure 4: Increasing water injection flow rates leads for all different fuels to enhanced electric performance.

heat capacity of the flue gases due to the combustion of hydrogen, this advantage disappears when the injected water flow rates increases. Indeed, this is obvious, considering that the specific water content of the flue gases, affecting the heat capacity, is affected much more by the water injection, canceling out this effect. Finally, for both cases, as maximal electric efficiency of 41.6% is reached.

Looking at the black box analysis for the different cases, it is apparent that the maximal water injection amount is not determined by the limitations set on the black box efficiency or destruction (Figure 5): For all cases, the exergy efficiency remains below 92% and the exergy destruction above 5%. Similar to previous observations, here again, the limit for water injection is determined by the compressor [9]. Considering that the turbine is choked, the mass flow rate entering this turbine is limited. When additional mass (here water) is added in the cycle behind the compressor, automatically the compressor will move its operating point towards lower rotational speed, pressure ratio and mostly lower mass flow rate, resulting in a reduction of surge margin. Hence, the limit for water injection is set by the compressor: the maximal water flow rates correspond to case with 0% surge margin (in practice, a minimal surge margin should still be respected).

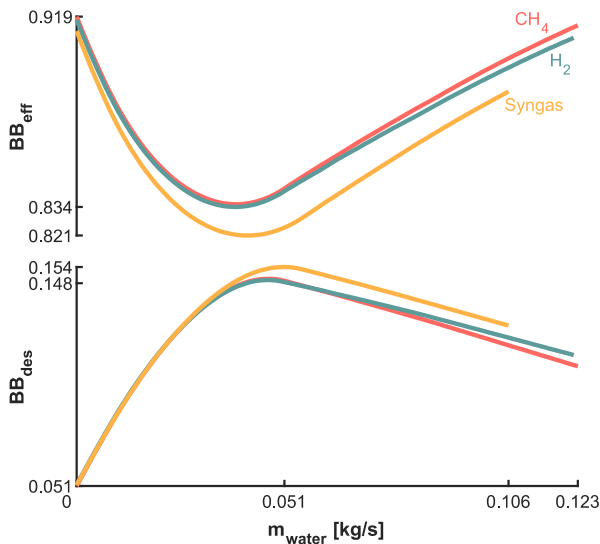


Figure 5: For all case, the black box efficiency (BB_{eff}) and destruction (BB_{des}) remain below the set limits.

For the evolution of the black box efficiency and destruction, we can observe reverse trends: first a reduction followed by an increase for the efficiency and first an increase followed by a decrease for the destruction. This particular behavior can be explained as follows: when more water is added in the cycle, despite a reduction in stack temperature, the total energy and

exergy content of the flue gases increases, due to the increased water vapor content. Once the temperature of the flue gases becomes significantly low, below the dewpoint (starting around 51 g/s of water injection), the large potential of evaporation enthalpy starts to be recovered, leading to increased exergy efficiency and reduced exergy destruction.

Finally, comparing the impact of the fuel alteration, again a major difference between the syngas and the methane and hydrogen cases can be observed. Again, due to the dilution when using syngas, larger exhaust gas flow rates can be observed in the syngas case, resulting in larger destruction and lower efficiency of exergy. For the hydrogen and the methane case, at first, only very small differences can be observed, considering that although in the hydrogen case, there is a higher vapor content in the flue gases, this difference is still limited. However, at higher mass flow rates of injected water, the relative difference in fraction becomes apparent to lead to some observable differences, e.g., 91.5% versus 90.9% exergy efficiency for the methane and hydrogen cases respectively. Nevertheless, as highlighted before, this leads to a negligible difference in electric efficiency.

To conclude the black box analysis, a comparison between the hot composite curves of the different cases is presented (Figure 6). It is remarkable to observe that there is no major difference between the different cases. Despite the constant TIT, TOT remains also rather unaffected (minor difference of 5°C). Moreover, the slopes of the different curves are rather similar, which can be explained by the large water fraction, cancelling out the impact of the different flue gas composition, as a result of the use of different fuels, on the heat capacity. Finally, the major difference between the syngas and the methane and hydrogen cases can be observed in the fact that more heat is exchanged in these later cases, leading to higher black box efficiencies, and linked electric efficiencies.

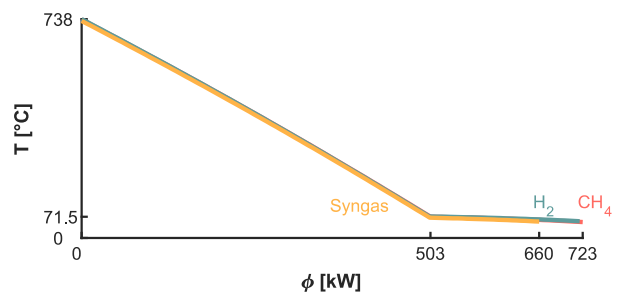


Figure 6: The hot composite curves show similar behavior for the different fuels.

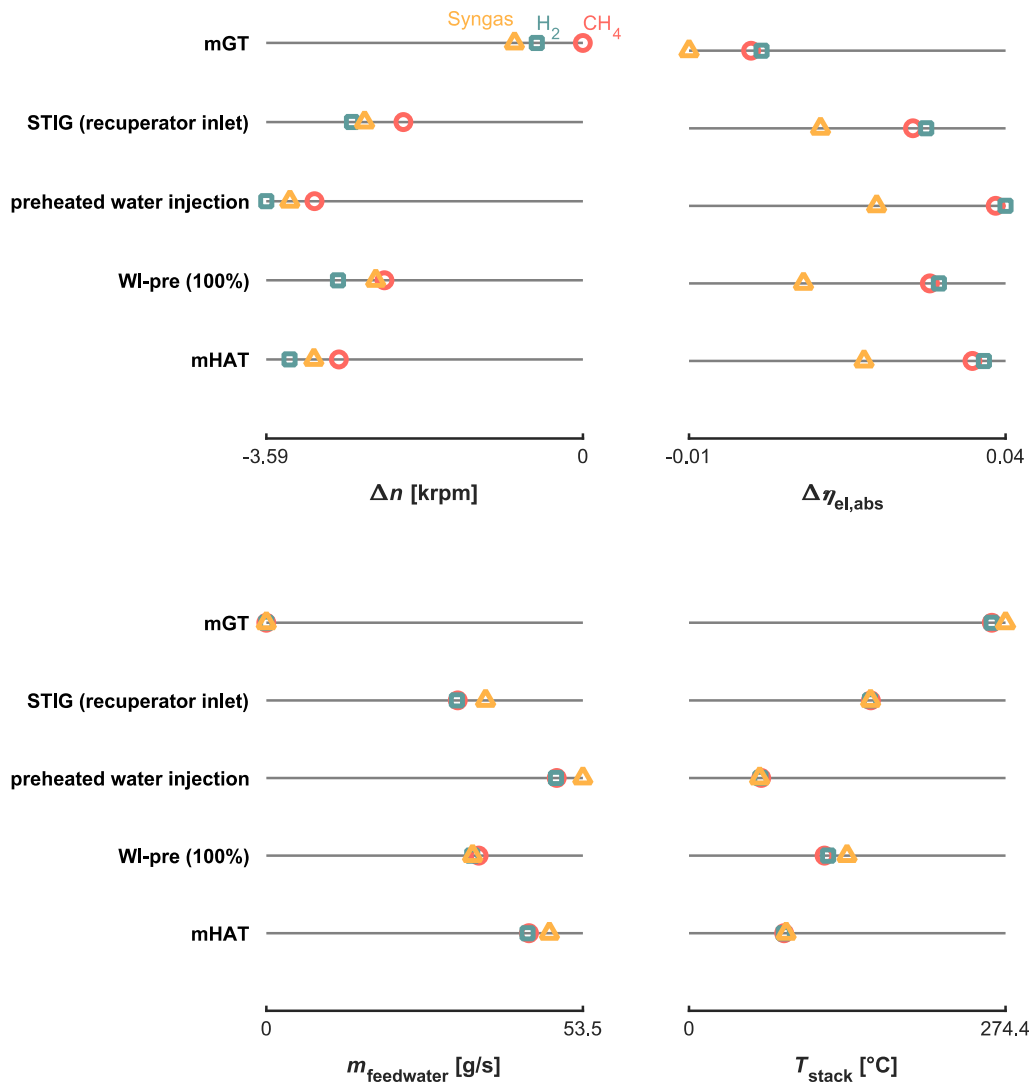


Figure 7: The preheated water injection case shows for all considered fuels the best performance, reflected by the higher water injection amount and lowest stack temperature. Simulations results are obtained considering constant TIT (950°C) and P_{el} (100 kW_e) and are compared with the dry mGT case running at CH₄ (Circles represent the CH₄ case, squares the H₂ case and the triangles the syngas cases).

3.3 Specific humidified mGT cycles.

Comparing the different specific humidified mGT cycles towards their potential for waste heat recovery through humidification, we can observe that the preheated water injection case shows the largest potential, for all different considered fuel cases, closely followed by the mHAT case (Figure 7). These cases also allow for the highest water introduction and thus highest waste heat recovery (reflected by the lowest stack temperature). These results are in line with previous findings [18]. When limiting the preheated water injection amount by the relative humidity of the compressed air (WI-pre (100%) case), we can observe that this has a rather negative impact on the cycle

performance. The heat recovery in the recuperator is strongly limited, even leading to lower performance than the STIG case.

Altering the fuel, as already highlighted before, has only a minor effect when switching from methane to hydrogen, while a major effect is reported for the syngas cases (negative impact). Switching to hydrogen has a slight positive impact on the electric efficiency for all cases, however, this is comparable to the slight increase in efficiency for the dry cycle. The invers trend at higher water injection rates, as observed in the black box case, where methane presented better performance is not observed here, considering that the amount of injected water is still rather limited in all cases (maximal 53.5 g/s), compared to the potential (123 g/s). For the syngas case,

despite a larger amount of injected water, the performance of the cycle is still worse than the methane and hydrogen case for all considered cycles. The dilution in the combustion chamber enables for more water introduction, but this is not reflected in higher electric performance. The difference between the specific humidified cases for syngas and methane and/or hydrogen are even larger than between the dry mGT, showing that in the case of syngas, less of the potential is used. Finally, it is worth to note that none of the cycles exploits the full potential, identified using the black box approach: indeed, none of the cycles is capable of recovering the large amount of condensation heat available at low temperature in the flue gases. As highlighted previously by the author of this paper, only by exploiting the M-power cycle, this full potential can be recovered, however, still requiring significantly high wet bulb effectiveness for the M-saturator of 98% [21].

4. CONCLUSIONS AND FUTURE WORK

In this paper, we studied the potential of humidified mGTs when using different fuels, both high (hydrogen) and low calorific (syngas) fuels, considering the necessary fuel diversification towards net zero-carbon emissions and future security of supply. To determine the impact of the fuel on this potential, both black box analysis and specific advanced humidified cycles have been simulated and assessed using Aspen Plus.

The black box analysis showed that altering between methane and hydrogen as fuel has no significant impact on the potential for cycle performance, while exploiting low calorific fuels leads to a significant reduction in potential. This potential is not set by the heat exchanger network itself (so not by the second law), but rather by the technical limitations of the compressor. A maximal injection of 122 g/s and 106 g/s for the respectively methane/hydrogen cases and syngas case were found, corresponding to a maximal efficiency of 41.7% and 38.7% respectively.

When considering specific cycle layouts, it was observed that the preheated water injection case, allowing two-phase flow in the recuperator, presents the highest efficiency increase of all cases for the 3 different fuels, followed by the mHAT cycle. Again, opting for hydrogen has a slight positive effect on the cycle performance, while syngas clearly leads to a negative impact.

Nevertheless, the presented efficiency was still significantly lower, for all case, than the identified black box potential, showing that more advanced cycles, allowing for the heat recovery of the low temperature evaporation heat in the flue gases, remain needed to exploit the full potential. Future work consists in the

extension of the current study towards the REVAP and M-power cycle, to identify their potential as well as the experimental validation of the predicted performance on actual humidified cycles operating on different fuels, e.g., H₂.

REFERENCE

- [1] U.S. Department of Energy, Office of Energy Efficiency and Renewable Energy, Office of Power Technologies. Advanced Microturbine Systems - Program plan for fiscal years 2000 through 2006. 2000.
- [2] Jonsson M, Yan J. Humidified gas turbines – a review of proposed and implemented cycles. *Energy*. 2005;30:1013-78.
- [3] De Paepe W, Montero Carrero M, Bram S, Parente A, Contino F. Toward Higher Micro Gas Turbine Efficiency and Flexibility—Humidified Micro Gas Turbines: A Review. *J Eng Gas Turbines Power Trans ASME*. 2018;140:081702 (9 pages).
- [4] Montero Carrero M, De Paepe W, Magnusson J, Parente A, Bram S, Contino F. Experimental characterisation of a micro Humid Air Turbine: assessment of the thermodynamic performance. *Appl Therm Eng*. 2017;118:796-806.
- [5] Hui Y, Wang Y, Weng S. Experimental investigation of pressurized packing saturator for humid air turbine cycle. *Appl Therm Eng*. 2014;62:513-9.
- [6] Montero Carrero M, De Paepe W, Bram S, Musin F, Parente A, Contino F. Humidified micro gas turbines for domestic users: an economic and primary energy savings analysis. *Energy*. 2016;117:429-38.
- [7] Stathopoulos P, Paschereit CO. Retrofitting micro gas turbines for wet operation. A way to increase operational flexibility in distributed CHP plants. *Applied Energy*. 2015;154:438-46.
- [8] Bram S, De Ruyck J. Exergy analysis tools for Aspen applied to evaporative cycle design. *Energy Convers Manage*. 1997;38:1613-24.
- [9] De Paepe W, Contino F, Delattin F, Bram S, De Ruyck J. Optimal waste heat recovery in micro gas turbine cycles through liquid water injection. *Appl Therm Eng*. 2014;70:846-56.
- [10] De Paepe W, Montero Carrero M, Bram S, Contino F, Parente A. Waste heat recovery optimization in micro gas turbine applications using advanced humidified gas turbine cycle concepts. *Applied Energy*. 2017;207:218-29.
- [11] Renzi M, Patuzzi F, Baratieri M. Syngas feed of micro gas turbines with steam injection: Effects on performance, combustion and pollutants formation. *Applied Energy*. 2017;206:697-707.
- [12] De Paepe W, Delattin F, Bram S, De Ruyck J. Steam injection experiments in a microturbine – A

thermodynamic performance analysis. *Applied Energy*. 2012;97:569-76.

[13] Parente J, Traverso A, Massardo AF. Micro Humid Air Cycle: Part B – Thermoeconomic Analysis. *ASME Conference Proceedings (ASME paper GT2003-38328)*. 2003;231-9.

[14] De Paepe W, Delattin F, Bram S, De Ruyck J. Water injection in a micro gas turbine – Assessment of the performance using a black box method. *Applied Energy*. 2013;113:1291-302.

[15] De Paepe W, Contino F, Delattin F, Bram S, De Ruyck J. New concept of spray saturation tower for micro Humid Air Turbine applications. *Applied Energy*. 2014;130:723-37.

[16] De Ruyck J, Bram S, Allard G. REVAP[®] Cycle: A New Evaporative Cycle Without Saturation Tower. *J Eng Gas Turbines Power Trans ASME*. 1997;119:893-7.

[17] Gillan L, Maisotsenko V. Maisotsenko open cycle used for gas turbine power generation. *ASME Turbo Expo 2003, collocated with the 2003 International Joint Power Generation Conference: American Society of Mechanical Engineers; 2003*. p. 75-84.

[18] De Paepe W, Carrero MM, Bram S, Contino F, Parente A. Waste heat recovery optimization in micro gas turbine applications using advanced humidified gas turbine cycle concepts. *Applied energy*. 2017;207:218-29.

[19] Parente J, Traverso A, Massardo AF. Micro Humid Air Cycle: Part A – Thermodynamic and Technical Aspects. *ASME Conference Proceedings (ASME paper GT2003-38326)*. 2003;2003:221-9.

[20] Rao AD. Process for producing power. US patent no. 4829763, 1989.

[21] De Paepe W, Pappa A, Montero Carrero M, Bricteux L, Contino F. Reducing waste heat to the minimum: Thermodynamic assessment of the M-power cycle concept applied to micro Gas Turbines. *Applied Energy*. 2020;279:115898.